Pergamon

*Int. J. Heat Mass Transfer.* Vol. 41, No. 2, pp. 347–356, 1998

Printed in Great Britain
0017–9310/98 $19.00+0.00

PII: S0017-9310(97)00146-4

# Transient non-Darcian forced convection flow in a pipe partially filled with a porous material

M. K. ALKAM and M. A. AL-NIMR†
Mechanical Engineering Department, Jordan University of Science and Technology, Irbid, Jordan

(*Received* 26 *November* 1996 *and in final form* 1 *May* 1997)

**Abstract**—In this paper, a numerical simulation is presented for the transient forced convection in the developing region of a cylindrical channel partially filled with a porous substrate. The porous substrate is attached to the inner side of the cylinder wall, which is exposed to a sudden change in temperature. The flow within the porous domain is modeled by the Brinkman–Forchheimer-extended Darcy model. The effects of several parameters on the hydrodynamic and thermal characteristics of the present problem are studied. These parameters include the porous substrate thickness, Darcy number and Forchheimer coefficient. Results of the current model show that the existence of the porous substrate may improve the Nusselt number at the fully developed region by a factor of 8. However, there is an optimum thickness of the porous substrate beyond which no significant improvement in the Nusselt number is achieved. Also, in the present work, the macroscopic inertial term in the porous domain momentum equation is included due to its significant effect. It is found that the steady state time increases as the substrate thickness increases up to a certain limit and then the steady state time decreases upon further increase in the substrate thickness. Also, increasing the Forchheimer coefficient and decreasing the Darcy number increase the steady state time. © 1997 Elsevier Science Ltd.

## INTRODUCTION

Convective heat transfer in channels partially filled with porous media has gained considerable attention in recent years because of its various applications in contemporary technology [1]. These applications include: porous journal bearing, blood flow in lungs or in arteries, nuclear reactors, porous-flat plate collectors, packed bed thermal storage, solidification of concentrated alloys, fibrous and granular insulation, grain storage and drying, paper drying, and food storage. Besides, the use of porous substrates to improve forced convection heat transfer in channels, which is considered as a composite of fluid and porous layers, finds applications in heat exchangers, electronic cooling, heat pipes, filtration and chemical reactors, etc. In these applications, engineers avoid filling the entire channel with a solid matrix to reduce the pressure drop.

Previous work on forced convection in composite fluid and porous layers is limited [2]. Using the simple Darcy model, the fluid mechanics at the interface between a fluid layer and a porous medium over a flat plate was first investigated by Beavers and Joseph [3]. Later, this problem was investigated by Vafai and Thiyagaraja [4] analytically. In their work, Vafai and Thiyagaraja obtained an approximate solution based on matched asymptotic expansions for the velocity and temperature distributions. In the work of Vafai and Thiyagaraja, the empirically-based correlation, used by Beavers and Joseph, was shown to be true for the linear regime which Beavers and Joseph had investigated. This correlation was verified by the development of an analytical model based on first principles, thereby showing that an extra matching condition is not needed. Vafai and Kim [2] presented an exact solution for the same problem. Excluding the microscopic (the Forchheimer or the microflow development) inertial term, closed form analytical solutions for parallel plates and circular pipes partially filled with porous materials were obtained by Poulikakos and Kazmierczak [5] for constant wall heat flux, while numerical results were computed for constant wall temperature. Jang and Chen [6] investigated the problem of forced convection in a parallel plate channel partially filled with a porous material numerically. In their work, Jang and Chen used the Darcy–Brinkman–Forchheimer model to describe the flow within the porous material. Also, they assumed a fully developed hydrodynamic behavior by excluding the macroscopic (or the macroflow development) inertial term and a steady state thermal behavior was considered. Rudraiah [7] applied different boundary conditions to the same problem using the Darcy–Brinkman model. Analytical solution was obtained by Chikh *et al.* [8] for the problem of forced convection under fully-developed hydrodynamic and steady thermal behavior in an annular duct partially filled with a porous medium. One of the annulus walls was exposed to isoflux and the other wall was insulated. The same problem, but with an isothermal boundary condition, was investigated numerically by the same group [9] using the Darcy–Brinkman–Forchheimer model.

† Author to whom correspondence should be addressed.

## NOMENCLATURE

$A$ coefficient of the microscopic inertia term, $\varepsilon Fr_2/\rho_R\sqrt{K}$
$c$ specific heat
$c_R$ heat capacity ratio, $\rho_2 c_2/\rho_1 c_1 = \varepsilon + (1-\varepsilon)\rho_s c_s/\rho_f c_f$
$Da$ Darcy number, $K/r_2^2$
$F$ Forchheimer coefficient, $1.8/(180\varepsilon^5)^{0.5}$
$k$ thermal conductivity
$k_R$ thermal conductivity ratio, $k_2/k_1$
$K$ permeability of the porous substrate
$N_1$ dimensionless radius ratio, $r_1/r_2$
$N_2$ $= 1$ dimensionless radius ratio, $r_2/r_2 = 1$
$Nu$ local Nusselt number, $hr_2/k_2 = \dfrac{\partial\theta_2}{\partial R}/(\theta_m - 1)$
$p$ pressure
$P$ dimensionless pressure, $pr_2^2/\rho_1 v_1^2$
$Pr$ Prandtl number of the fluid, $c_1\mu_1/k_1$
$r$ radial coordinate
$r_1$, $r_2$ interface and outer radii of annulus
$R$ dimensionless radial coordinate, $r/r_2$
$t$ time
$t_{ss}$ steady state time
$T$ temperature at any point
$T_i$ initial temperature
$T_m$ mixing cup temperature over any cross section $(\int_0^{r_1} ru_1 T_1\,dr + \int_{r_1}^{r_2} ru_2 T_2\,dr)/(\int_0^{r_1} ru_1\,dr + \int_{r_1}^{r_2} ru_2\,dr)$
$T_0$ temperature of heat transfer boundary
$u$ axial velocity
$u_0$ inlet axial velocity
$U$ dimensionless volume averaged axial velocity, $ur_2/v_1$
$U_0$ dimensionless inlet axial velocity, $u_0 r_2/v_1$
$v$ radial velocity
$V$ dimensionless radial velocity, $vr_2/v_1$
$z$ axial coordinate
$z_{en}$ hydrodynamic entrance length
$Z$ dimensionless axial coordinate, $z/r_2$
$Z_{en}$ dimensionless hydrodynamic entrance length, $z_{en}/r_2$.

Greek symbols

$\varepsilon$ porosity
$\theta$ dimensionless temperature $(T-T_i)/(T_0-T_i)$
$\theta_m$ dimensionless mixing cup temperature $(T_m-T_i)/(T_0-T_i)$
$\mu$ dynamic viscosity
$\mu_2$ effective dynamic viscosity of the porous domain
$\mu_R$ dynamic viscosity ratio, $\mu_2/\mu_1$
$\nu$ kinematic viscosity
$\nu_R$ kinematic viscosity ratio, $\nu_2/\nu_1$
$\rho$ density
$\rho_R$ density ratio, $\rho_2/\rho_1$
$\tau$ dimensionless time, $tv_1/r_2^2$
$\tau_{ss}$ dimensionless steady state time, $t_{ss}v_1/r_2^2$.

Subscripts

1 or f fluid domain properties
2 porous domain properties
R ratio
s solid matrix properties
ss steady state.

The investigations cited above are concerned with steady state forced convection problems in different composite geometries. All the models presented by these investigations drop the macroscopic inertial force from the momentum governing equations according to the assumption of fully developed hydrodynamics. However, and as reported by Vafai and Kim [10], and Al-Nimr and Alkam [11], the macroscopic inertial term has significant effects especially on the thermal behavior in channels partially filled with porous material. Including the macroscopic inertial term in the governing equations is essential to ensure the matching between the flow development in the clear fluid and in the fluid-saturated porous layer.

In the present work, the transient forced convection in circular channels partially filled with porous materials is numerically simulated. The transient behavior in the thermal field is caused by a step temperature change at the cylinder wall. The hydrodynamic flow characteristics are assumed to be steady, but in developing situations. The interactions between the porous medium and the clear fluid is simulated by the Darcy–Brinkman–Forchheimer formulation and the continuity of velocity and stresses at the interface [10]. The effects of several parameters, such as the porous layer thickness, the system configuration, Forchheimer coefficient, and Darcy number are investigated. The study includes the effect of these parameters on the transient thermal behavior of the channel under consideration.

## MATHEMATICAL FORMULATION

The physical problem under consideration consists of a circular cylinder as shown in Fig. 1. A porous substrate is deposited at the cylinder wall. The heating (or cooling) process is in the form of a sudden change in the boundary-temperature. Both the fluid and the solid matrix have constant physical properties, and the fluid enters the circular passage with a uniform

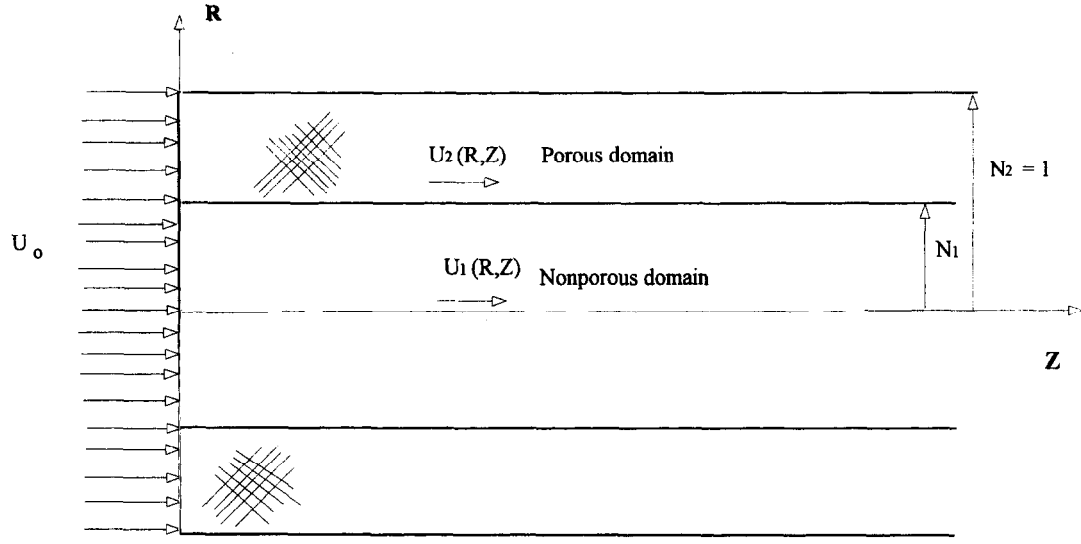


Fig. 1. Schematic diagram of the problem under consideration.

velocity distribution, $u_0$, which is independent of time. Prior to the start of the time varying heating (or cooling) process, the fluid may either be in a thermal steady-state as a result of some steady heating process, or alternatively, the fluid and the channel wall may be at the same uniform temperature. The transient forced convection process starts by imposing (at $\tau > 0$) a sudden change in the temperature of the cylinder wall.

The current investigation has been carried out assuming axisymmetric, laminar, boundary-layer flow with no internal heat generation, and neglecting viscous dissipation and axial conduction of heat. Also, it is assumed that the porous medium is homogeneous, isotropic and saturated with a single-phase. The fluid is in local thermal equilibrium with the solid matrix. Using the dimensionless parameters given in the nomenclature, the equations of continuity, motion, and energy, for both fluid and porous domains, reduce to the following non-dimensional equations, respectively

$$\frac{\partial U_1}{\partial Z} + \frac{1}{R}\frac{(R\partial V_1)}{\partial R} = 0 \tag{1}$$

$$\frac{\partial U_2}{\partial Z} + \frac{1}{R}\frac{(R\partial V_2)}{\partial R} = 0 \tag{2}$$

$$U_1\frac{\partial U_1}{\partial Z} + V_1\frac{\partial U_1}{\partial R} = -\frac{\partial P}{\partial Z} + \frac{1}{R}\frac{\partial}{\partial R}\left[R\frac{\partial U_1}{\partial R}\right] \tag{3}$$

$$U_2\frac{\partial U_2}{\partial Z} + V_2\frac{\partial U_2}{\partial R} = -\frac{1}{\rho_R}\frac{\partial P}{\partial Z} + \frac{\nu_{R,e}}{R}\frac{\partial}{\partial R}\left[R\frac{\partial U_2}{\partial R}\right] - \frac{1}{\rho_R Da}U_2 - AU_2^2 \tag{4}$$

$$\frac{\partial \theta_1}{\partial \tau} + U_1\frac{\partial \theta_1}{\partial Z} + V_1\frac{\partial \theta_1}{\partial R} = \frac{1}{Pr_1}\frac{1}{R}\frac{\partial}{\partial R}\left[R\frac{\partial \theta_1}{\partial R}\right] \tag{5}$$

$$C_R\frac{\partial \theta_2}{\partial \tau} + U_2\frac{\partial \theta_2}{\partial Z} + V_2\frac{\partial \theta_2}{\partial R} = \frac{k_R}{Pr_1}\frac{1}{R}\frac{\partial}{\partial R}\left[R\frac{\partial \theta_2}{\partial R}\right]. \tag{6}$$

In equations (1)–(6), subscripts 1 and 2 refer to the clear fluid and porous substrate, respectively. It should be pointed out that it is uncertain what one should use for the effective viscosity ratio $\mu_{R,e}$. Although the suitable value of $\mu_{R,e}$ is far from being settled, the viscosity ratio is taken as either unity or $1/\varepsilon$ in the heat transfer literature [1]. In fact, $\mu_{R,e} = 1$ is a good approximation in the range $0.7 \leqslant \varepsilon \leqslant 1$. For lower porosity, the use of the Einstein equation [13] for the viscosity of dilute suspension leads to a value of effective viscosity greater than the fluid viscosity. Also, it is noteworthy that the radial momentum equation has been eliminated due to the boundary-layer simplifications. However, it is possible, under the linearized numerical scheme of Bodoia and Osterle [12], to compensate for the lack of such an equation by using the following dimensionless integral continuity equation:

$$\int_0^{N_1} U_1 R\,dR + \int_{N_1}^{1} U_2 R\,dR = \frac{U_0}{2}. \tag{7}$$

In the case under consideration, the momentum equations assume the following boundary conditions:
at $Z = 0$ and $0 < R < 1$

$$U_1 = U_2 = U_0 \quad \text{and} \quad V_1 = V_2 = 0 \tag{8}$$

for $Z > 0$ and $R = 1$

$$U_2 = V_2 = 0$$

for $Z > 0$ and $R = 0$

$$\frac{\partial U_1}{\partial R} = 0$$

for $Z > 0$ and $R = N_1$

$$U_1 = U_2, \quad \frac{\partial U_1}{\partial R} = \mu_{R,e} \frac{\partial U_2}{\partial R}.$$

The energy equations have the following initial conditions:

$$\text{at } \tau = 0 \quad \theta_1 = \theta_2 = 0. \tag{9}$$

For $\tau > 0$, the thermal boundary conditions for the considered case are:
at $R = 0$

$$[\frac{\partial \theta_1}{\partial R} = 0 \tag{10}$$

and at $R = 1$

$$\theta_2 = 1.$$

The thermal conditions at the duct inlet and at the interface between the fluid and the porous domains are:
at $Z = 0, \quad 0 < R < 1$

$$\theta_1 = \theta_2 = 0$$

at $Z > 0, \quad R = N_1$

$$\theta_1 = \theta_2 \quad \text{and} \quad \frac{\partial \theta_1}{\partial R} = k_R \frac{\partial \theta_2}{\partial R}. \tag{11}$$

## NUMERICAL METHOD OF SOLUTION

In the present work, there are three independent variables: $R$, $Z$ and $\tau$. A three-dimensional parallel piped grid in $R$, $Z$ and $\tau$ has been imposed on half of the cylindrical flow field due to symmetry about the $Z$-axis. The non-dimensional time, $\tau$, is simulated as a third coordinate, normal to the $R$–$Z$ plane. The linearized implicit finite difference equations are derived using second-order central difference scheme for the radial derivatives, and first-order backward scheme for both the axial and time derivatives. The consistency and stability of the discretized governing equations have been checked, and it is found that the derived forms are consistent and stable as long as the downstream axial velocities $U_1$ and $U_2$ are non-negative, i.e. there is no flow reversal within the domain of the solution.

The method discussed by Bodoia and Osterle [12, 14] is used to solve the finite difference equations that simulate the flow hydrodynamics at steady state conditions. Having obtained the values of $U_1$, $U_2$, $V_1$ and $V_2$ over the flow field, the discretized energy equations are solved by marching in time. The solution procedure in time is carried out until steady-state conditions are practically achieved. The steady-state conditions are declared when the summation of the residue over the cross-section reaches a value less than $1 \times 10^{-4}$. The residue is defined as the absolute difference in temperature between a grid point and the previous one in time direction.

In order to obtain a solution independent of the grid size, several runs were performed to obtain the optimum step sizes in $R$, $Z$ and $\tau$ directions. The optimization of the grid size includes computing the radial temperature distribution at an arbitrary location, employing a given number of grid points in both the radial and axial directions. After that the number of grid points is increased gradually, and each time, a computer run is performed to compute the temperature profiles. A residue is defined as the absolute difference in temperature between the computed temperature distribution and the one obtained in the previous run. The procedure is continued until the residue approaches a value less than $1 \times 10^{-4}$. At this point the spatial grid size is fixed. Similar procedure is followed to choose the optimum time step. The optimum choice was $\Delta R = 0.02$, $\Delta Z = 0.1$, and $\Delta \tau = 0.01$.

## RESULTS AND DISCUSSION

The computations are carried out for the following typical values of the flow and geometry parameters:

$$Pr_1 = 0.7, k_R = 5, \mu_R = 1, \rho_R = 2, c_R = 1, U_0 = 100.$$

In order to validate the present code, a special computer run was made in which $Da \to \infty$, $A \to 0$ and $N \to 1$. These operating conditions represent the flow of a fluid in a clear tube. The obtained fully developed axial velocity distribution and the results are shown in Fig. 2. The difference between the obtained numerical and analytical results is insignificant.

Figure 3 shows the axial velocity distribution in the radial direction at different axial locations $Z$. This figure shows that the mean fluid velocity in the porous domain is lower than that in the clear domain. This is due to the additional retardation of the flow caused by the microscopic inertial and viscous forces generated by the porous solid matrix. Also, the fluid mean velocity in the porous domain decreases as one marches downstream. The drafted fluid from the porous region enhances the fluid flow in the clear domain and causes an increase in its average maximum velocity.

Figure 4 shows the dynamic variation in the radial temperature distribution. The figure suggests that external heating, which is applied on the cylinder boundary, has more effective penetration in the porous substrate than that in the clear fluid domain. This is due to the improvement in Nusselt number as will be shown later.

The effect of the porous substrate thickness on the axial variation of $Nu$ number is shown in Fig. 5. As shown from this figure, increasing the substrate thickness improves the fully developed $Nu$ number up to 8 times. The effect of the porous substrate thickness on the fully developed $Nu$ under steady state conditions,

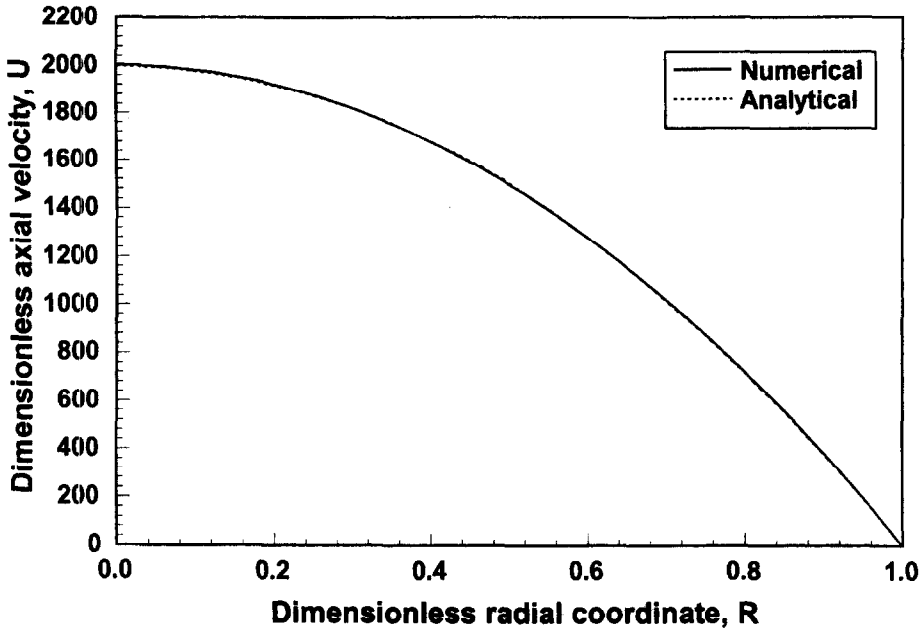


Fig. 2. A comparison between numerical and analytical results for code verification. The case shown presents the steady state, fully developed flow in a nonporous pipe.

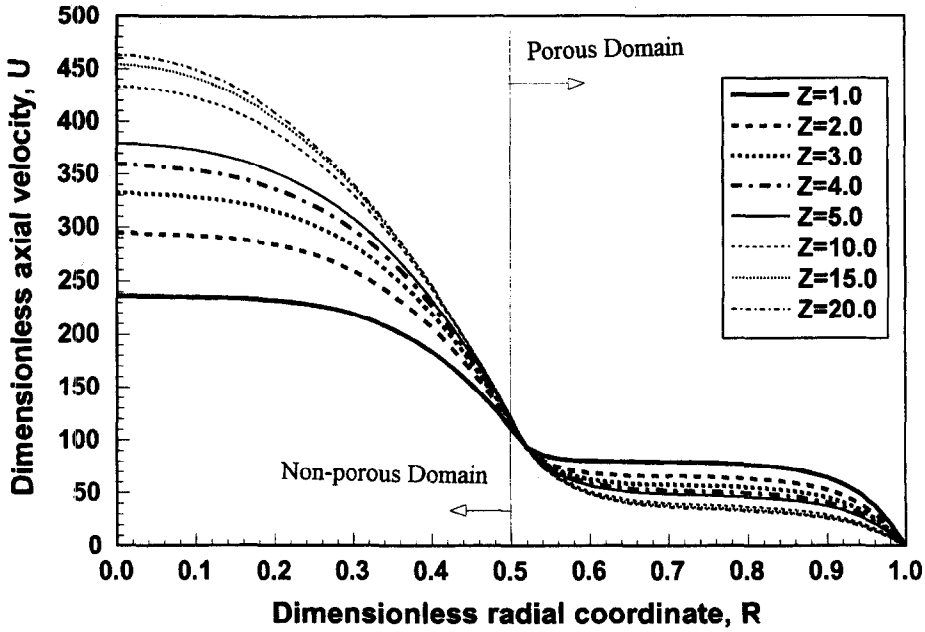


Fig. 3. Axial velocity distribution in the radial direction at different axial locations. $A = 1.0$ and $Da = 0.01$.

is shown in Fig. 6. Increasing the porous substrate thickness (decreasing $N_1$) causes a substantial increase in $Nu$ especially at higher values of $A$. The improvement in $Nu$ due to the porous substrate is caused by: (1) the substrate role in enhancing the mixing mechanism between the fluid and the wall, (2) increasing the fluid effective thermal conductivity, and (3) producing a thinner hydrodynamic boundary layer (low thermal resistance). The results of Fig. 6 are replotted from another point of view in Fig. 7. It is shown that $A$, in the considered range, has no significant effects on $Nu$ for the entire range of the substrate thickness.

The effect of $Da$ number on $Nu$ number and for different substrate thicknesses is shown in Fig. 8. For large $Da$ number, increasing the porous substrate thickness increases $Nu$ number as mentioned previously. However, for very small $Da$ numbers, increasing the porous substrate thickness leads to a small reduction in $Nu$ number. Very small $Da$ numbers

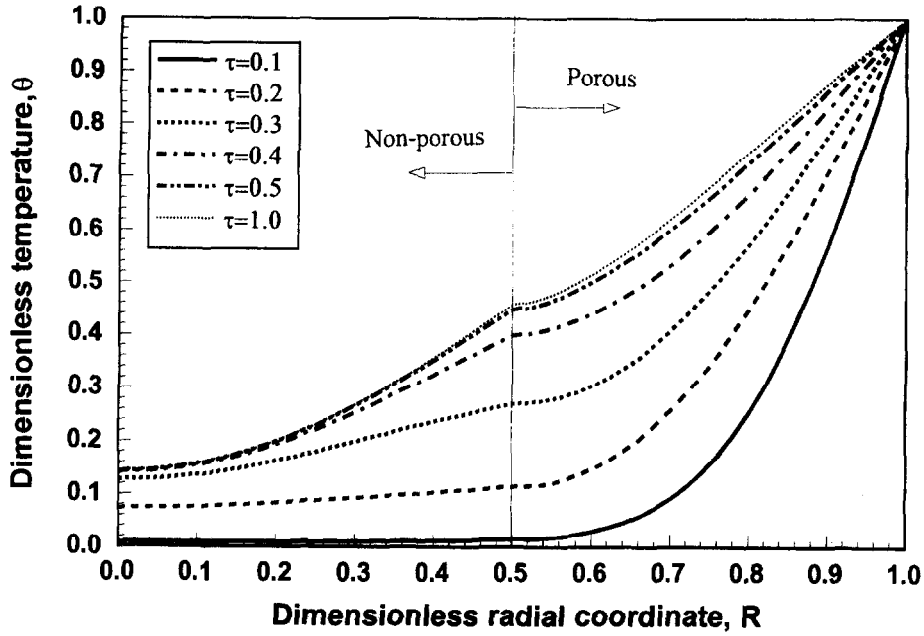


Fig. 4. Transient temperature distribution in the radial direction. $Z = 20$. $N1 = 0.5$, $A = 1.0$ and $Da = 0.01$.

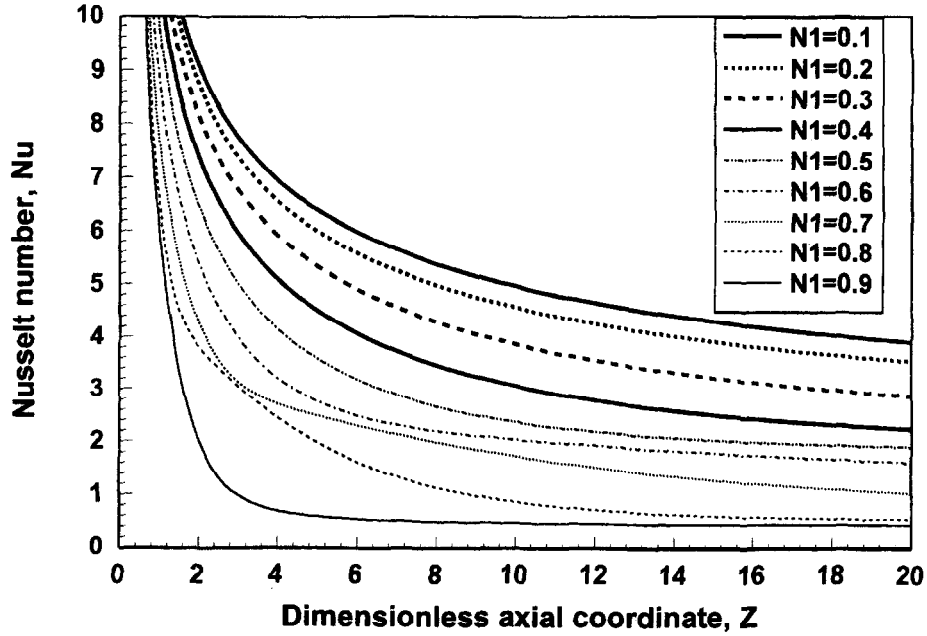


Fig. 5. axial variation of Nusselt number at steady-state conditions. $Da = 0.01$ and $A = 1$.

implies substrates of small permeability. This means that the substrate behaves nearly as a complete solid layer which does not contain any voids. In this case increasing the substrate thickness increases the thermal insulation and reduces the *Nu* number. Also, Fig. 8 shows that *Da* number has insignificant effect on *Nu* number for substrates of small thicknesses. In the limit $N_1 \to 1$, the system does not recognize the existence of a very small substrate thickness. Also, it is clear from Fig. 8 that there are two critical limits for *Da* number before and beyond which the variation in *Nu* number is insignificant. As clear from the porous domain momentum equation, the momentum equation does not recognize variations in large values of *Da* numbers. Also, very small *Da* numbers imply that substrates contain a complete solid, with no or with small voids, and as a result, $U_2 \approx 0$. Very small velocities eliminate the effect of *Da* number. In this limit, small values of *Nu* number result from pure conduction.

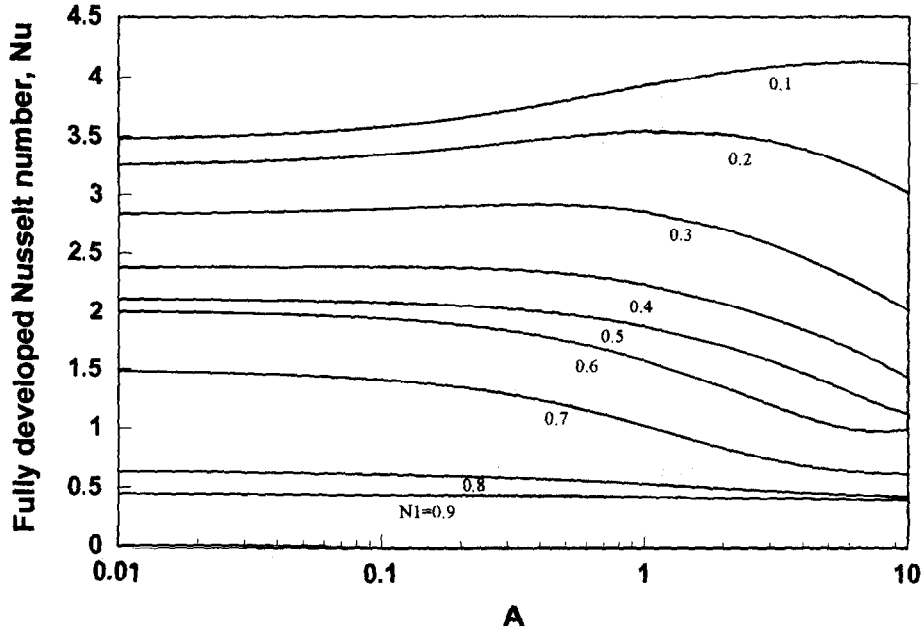


Fig. 6. Effect of Forchheimer number on the fully developed Nusselt number at steady-state conditions for different substrate thicknesses. $Da = 0.01$.

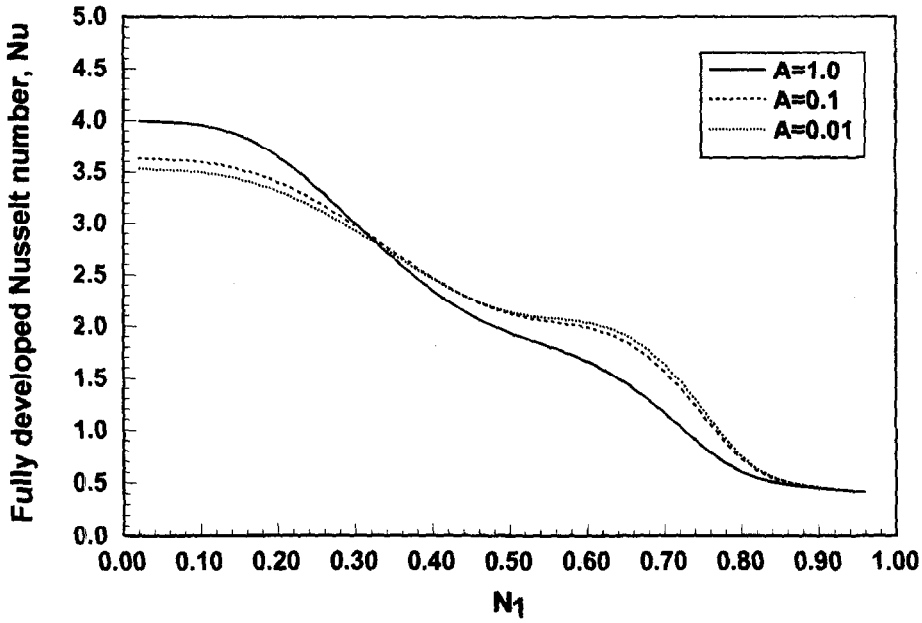


Fig. 7. Effect of substrate thickness on the fully-developed Nusselt number at steady-state conditions for different Forchheimer numbers. $Da = 0.01$.

Figure 9 shows the axial variation in the steady state time $\tau_{ss}$, which is the time required to attain steady state thermal behavior at certain location, for different porous substrate thicknesses. As shown from this figure, locations far away from the entrance need larger time to attain the steady state thermal behavior due to their low $Nu$ numbers. Also, it is clear that increasing the porous substrate thickness from $N_1 = 1$ (or $N_1 = 0.9$) to $N_1 = 0.5$, increases $\tau_{ss}$. This is due to the increase in the total thermal capacity of the domain that results from the increase in the solid matrix mass. It is important to note here that the increase in the porous substrate thickness or the reduction in the solid matrix void ratio has no effect on the volumetric flow rate within the channel. This is due to imposing the continuity condition which ensures that the volumetric flow rate within the channel is constant. The increase in $\tau_{ss}$ occurs in spite of

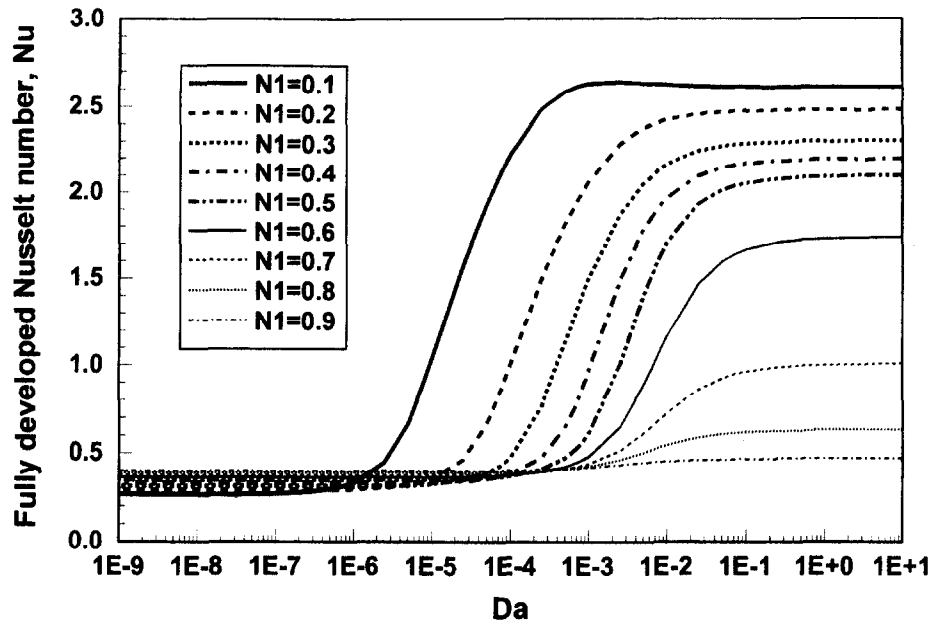


Fig. 8. Effect of *Da* number on the fully developed Nusselt number at steady-state conditions for different substrate thicknesses. $A = 1.0$.

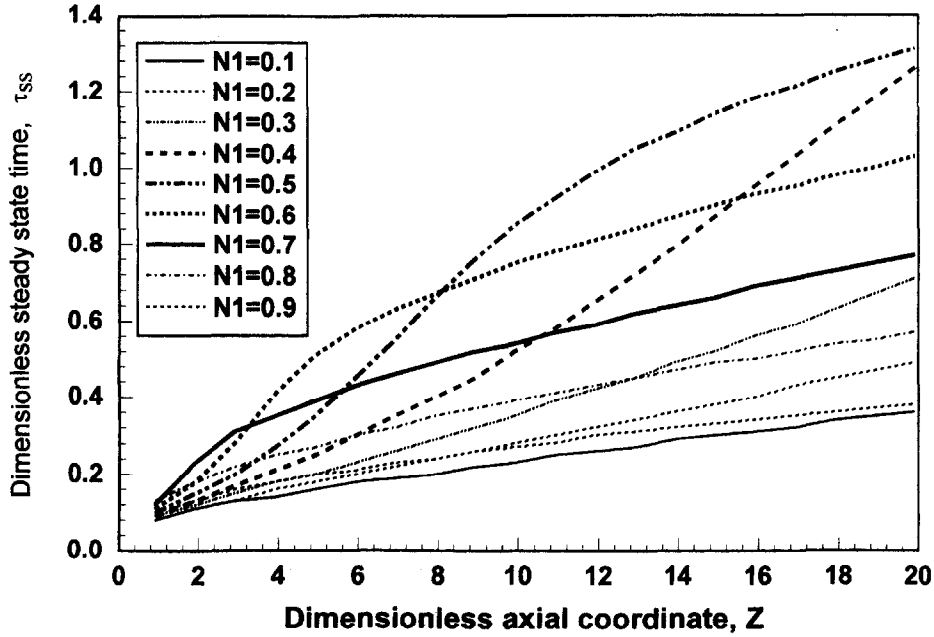


Fig. 9. Effect of substrate thickness on the axial variation of the steady-state time. $Da = 0.01$, $A = 1.0$.

the improvement in *Nu* number which resulted from increasing the porous substrate thickness. The small enhancement in the heat absorbed from the wall, due to the improvement in *Nu* number is overcome by the significant increase in the total thermal capacity of the system which is proportional to $N_1^2$. Further increase in the porous substrate thickness (from $N_1 = 0.5$ to $N_1 = 0$) leads to a significant reduction in $\tau_{ss}$. Increasing the substrate thickness in this range brings insignificant increase in the system thermal capacity (since the thermal capacity is proportional to $N_1^2$) and as a result, the small improvement in *Nu* number overcomes the insignificant increase in the thermal capacity of the system resulting from increasing the porous substrate thickness.

The effect of *Da* number on the axial variation in $\tau_{ss}$ is shown in Fig. 10. As shown in this figure, increasing *Da* number leads to significant reduction in $\tau_{ss}$. The Darcy number may be increased by using porous substrate of large permeability. The permeability of a

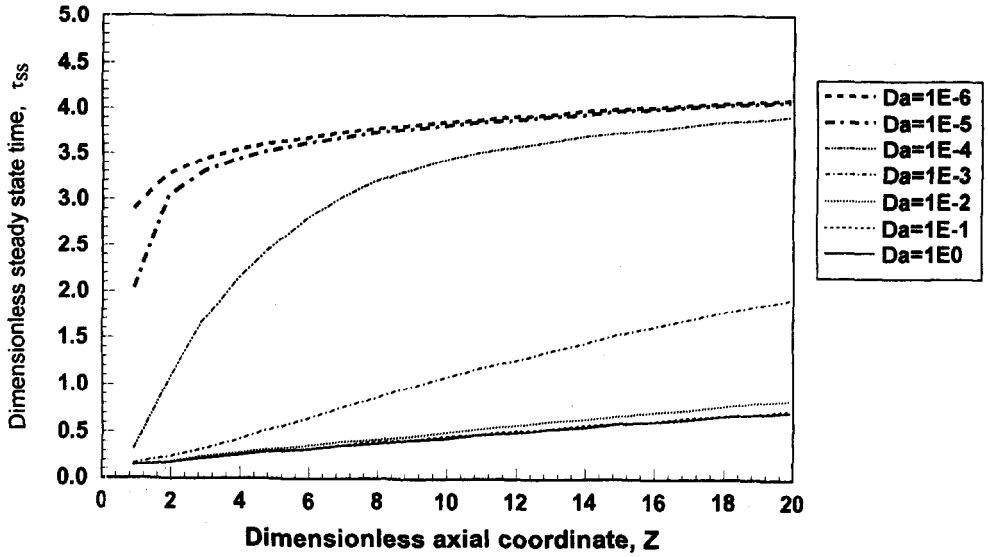


Fig. 10. Effect of *Da* number on the axial variation of the steady-state time. $N1 = 0.5$, $A = 1.0$.

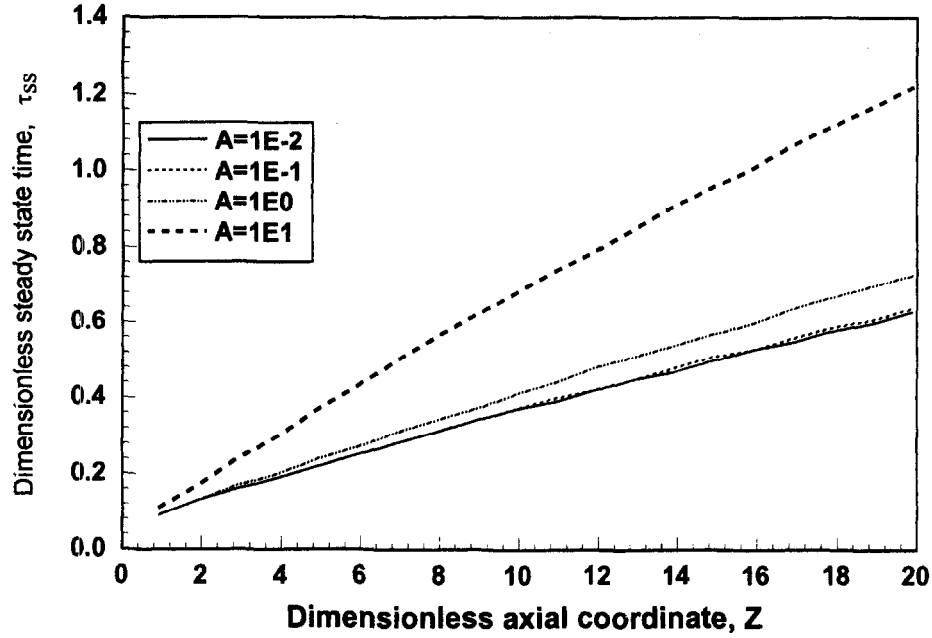


Fig. 11. Effect of Forchheimer number on the axial variation of the steady-state time $N1 = 0.5$, $Da = 0.01$.

given porous domain is a strong function of its porosity and it increases by increasing the void ratio of the porous domain. Light porous domains (of large void ratio) have low thermal capacity which in turn have small $\tau_{ss}$. Also, it is clear from Fig. 10 that large *Da* numbers have insignificant effect on $\tau_{ss}$. In the range of large *Da* numbers, the small reduction in the void ratio, which leads to a small increase in the system thermal capacity, is overcome by the improvement in the *Nu* number.

Figure 11 shows the effect of the microscopic inertial term (Forchheimer term) on the axial variation of $\tau_{ss}$. As *A* increases, the steady-state time increases. The coefficient of the microscopic inertial term may be increased by using solid matrix of low permeability. Such a matrix has small void ratio. As the void ratio decreases, the density of the solid matrix increases, and as a result, its thermal capacity increases, which in turn increases $\tau_{ss}$.

## CONCLUSIONS

Numerical solutions are presented for the problem of transient developing forced convection flow in circular channels partially filled with porous substrates. Including the macroscopic inertial term, the Brinkman–Forchheimer-extended Darcy model is used to model the flow inside the porous domain. The effects

of different parameters regarding the geometry, the solid matrix, and the fluid on the hydrodynamic and thermal behavior are investigated.

It is concluded that porous substrates may improve Nusselt number up to eight times. The effect of the microscopic inertial term, $A$, on $Nu$ number is found to be insignificant. On the other hand, large values of $Da$ numbers have significant effects on the fully developed $Nu$ number and especially for substrates of large thicknesses. Also, it is found that increasing the substrate thickness increases the steady-state time up to a certain limit and then it decreases for further increase in the substrate thickness. Increasing the Forchheimer coefficient and decreasing Darcy number increase the steady-state time.

## REFERENCES


1. Kakac, S., Kilkis, B., Kulacki, F. and Arinc, F., *Convective Heat and Mass Transfer in Porous Media*. Kluwer Academic Publishers, Netherlands, 1991, pp. 563–615.
2. Vafai, K. and Kim, S. J., Fluid mechanics of the interface region between a porous medium and a fluid layer—an exact solution. *International Journal of Heat and Fluid Flow*, 1990, **11**, 254–256.
3. Beavers, G. S. and Joseph, D. D., Boundary conditions at a naturally permeable wall. *Journal of Fluid Mechanics*, 1967, **13**, 197–207.
4. Vafai, K. and Thiyagaraja, R., Analysis of flow and heat transfer at the interface region of a porous medium. *International Journal of Heat and Mass Transfer*, 1987, **30**, 1391–1405.
5. Poulikakos, D. and Kazmierczak, M., Forced convection in a duct partially filled with a porous material. *ASME Journal of Heat Transfer*, 1987, **109**, 653–662.
6. Jang, J. Y. and Chen, J. L., Forced convection in a parallel plate channel partially filled with a high porosity medium. *International Communication of Heat and Mass Transfer*, 1992, **19**, 263–273.
7. Rudraiah, N., Forced convection in a parallel plate channel partially filled with a porous material. *ASME Journal of Heat Transfer*, 1985, **107**, 322–331.
8. Chikh, S., Boumedien, A., Bouhadef, K. and Lauriat, G., Analytical solution of non-Darcian forced convection in an annular duct partially filled with a porous medium. *International Journal of Heat and Mass Transfer*, 1995, **38**, 1543–1551.
9. Chikh, S., Boumedien, A., Bouhadef, K. and Lauriat, G., Non-Darcian forced convection analysis in an annular partially filled with a porous material. *Numerical Heat Transfer A*, 1995, **28**, 707–722.
10. Vafai, K. and Kim, S. J., On the limitations of the Brinkman–Forchheimer-extended Darcy equation. *International Journal of Heat and Fluid Flow*, 1995, **16**, 11–15.
11. Al-Nimr, M. A. and Alkam, M., Transient-non-Darcian forced convection analysis in an annulus partially filled with a porous material. Accepted for publication in the ASME Journal of Heat Transfer, 1997.
12. Bodoia, J. R. and Osterle, J. F., Finite-difference analysis of plane poiseuille and couette flow developments. *Applied Science Research*, 1961, **A10**, 265–276.
13. Kaviany, M., *Principles of Heat Transfer in Porous Media*, 2nd edn. Springer, New York, 1995, p. 52.
14. El-Shaarawi, M. A. and Alkam, M. K., Transient forced convection in the entrance region of concentric annuli. *International Journal of Heat and Mass Transfer*, 1992, **35**, 3335–3344.